International Journal of Science and Research (IJSR)
ISSN (Online): 2319-7064
Index Copernicus Value (2013): 6.14 | Impact Factor (2013): 4.438

Finite Element Analysis of Friction Welding Process for 2024Al Alloy and UNS C23000 Brass

V. Srija[1], A. Chennakesava Reddy[2]

PG student, Department of Mechanical Engineering, JNTUH College of Engineering, Kukatpally, Hyderabad – 500 085, Telangana, India

Professor, Department of Mechanical Engineering, JNTUH College of Engineering, Kukatpally, Hyderabad – 500 085, Telangana, India

Abstract: ***The purpose of this work was to weld dissimilar metals of 2024Al and brass by continuous drive friction welding. The finite element analysis has been carried out to model the continuous drive friction welding. The process parameters have been optimized using Taguchi techniques. The optimal process parameters for 2024Al and brass are found to be frictional pressure of 40 MPa, frictional time of 4 sec, rotational speed of 1500 rpm and forging pressure of 37.5 MPa.***

Keywords: 2024Al, UNS C23000 brass, finite element analysis, Taguchi, continuous drive friction welding.

1. Introduction

Friction welding is a solid-state welding process that allows material combinations to be joined than with any other welding process. In continuous drive friction welding, one of the workpieces is attached to a motor driven unit while the other is restrained from rotation as showed in figure 1a. The motor driven workpiece is rotated at a predetermined constant speed. The workpieces to be welded are forced together and then a friction force is applied as shown in figure 1b. Heat is generated because of friction between the welding surfaces. This is continued for a predetermined time as showed in figure 1c. The rotating workpiece is halted by the application of a braking force. The friction force is preserved or increased for a predetermined time after the rotation is ceased (figure1d). Figure1also illustrates the variation of welding speed, friction force and forging force with time during various stages of the friction welding process.

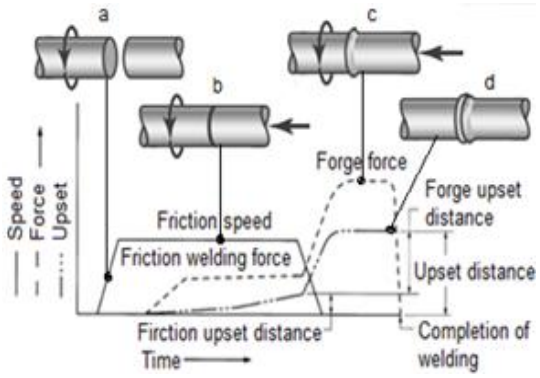

Figure 1: Friction welding

Even metal combinations not normally considered compatible can be joined by friction welding, such as aluminum to steel, copper to aluminum, titanium to copper and nickel alloys to steel. As a rule, all metallic engineering materials which are forgeable can be friction welded, including automotive valve alloys, maraging steel, tool steel, alloy steels and tantalum [1, 2]. With friction welding, joints are possible between not only two solid materials or two hollow parts, but also solid material/hollow part combinations can be reliably welded. However, the shape of a fusion zone in friction welding is dependent the frictional pressure and the rotational speed. If the applied force is too high or the rotational speed is too low, the fusion zone at the centre of the joint will be narrow as showed in figure 2a. On the other hand, if the applied force is too low or the rotational speed is too high, the fusion zone at the centre of the joint will be wider as showed in figure 2b. In both the cases, the result is poor weld joint strength.

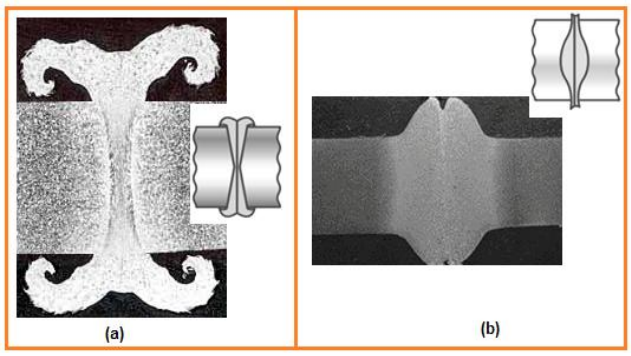

Figure 2: Effect of frictional pressure and rotational speed in friction welding

In the friction welding process, the developed heat at the interface raises the temperature of workpieces rapidly to values approaching the melting range of the material. Welding occurs under the influence of pressure that is applied when heated zone is in the plastic range, as mentioned [3]. The foremost difference between the welding of similar materials and that of dissimilar materials is that the axial movement is unequal in the latter case whilst the similar materials experience equal movement along the common axis. This problem arises not only from the different coefficients of thermal expansion, but also from the distinct hardness values of the dissimilar materials to be joined. Joint and edge preparation is very important to produce distortion free welds. The solid-state diffusion is slow in the wider joints [4].The intermetallic compounds can change the micro hardness near the joint interface of dissimilar metals [5].

As aluminum–copper welds for power transmission applications are likely to be functional rather than structural, electrical rather than mechanical properties are likely to be of

greater importance. Therefore, friction welding of dissimilar metals needs to be eased by ensuring that both the workpieces deform similarly. In this context, this research work aims at finite element analysis of friction welding process for aluminum (2024A) and UNS C23000 brass with underlying background:

1. The microstructure is known to affect electrical properties with smaller grain sizes (increased volume fraction of grain boundaries), increased solute concentrations and increased lattice defects (dislocations), increasing resistivity. All of these entities act as scattering centers and therefore impede the flow of current across the sample.
2. The temperature of welding increases resistivity, with higher sample temperatures increasing lattice vibrations and therefore increasing scattering.
3. Aluminum–copper intermetallics have much higher resistivity than either of the parent metals, and therefore, the presence of these intermetallics could cause excessive resistance and unwanted heating at the weld line. This could be important as there are requirements for bus bars to be kept below certain temperatures during operation.

2. Finite Element Modeling

In this study, ANSYS workbench (15.0) software was used in the coupled deformation and heat flow analysis during friction welding of UNS C23000 brass and aluminum (2024Al). An axisymmetric 3D model [6] of aluminum (2024Al) - UNS C23000 brass rods of 25.4 mm diameter and 100 mm length was made using ANSYS workbench as shown in figure 3. Hexahedron elements [7] were used to mesh the aluminum and brass rods. The rotating part was modeled with 3298 elements and 14904 nodes and the non-rotating part was meshed with 16493 nodes and 3672 elements.

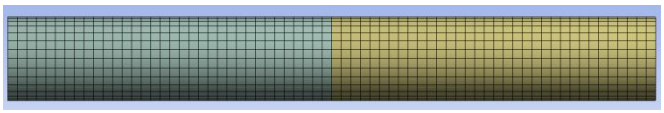

Figure 3: Finite element modeling of friction welding

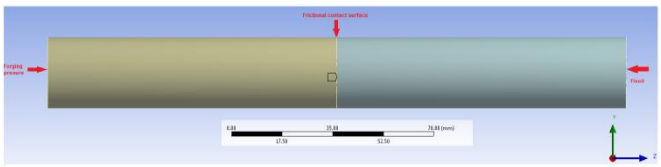

Figure 4: The boundary conditions

The boundary conditions are mentioned in figure 4. First the transient thermal analysis was carried out keeping brass rod stationary and aluminum rod in rotation. The coefficient of friction 0.2 was applied at the interface of brass and aluminum rods. The convection heat transfer coefficient was applied on the surface of two rods. The heat flux calculations were imported from ANSYS APDL commands and applied at the interface. The temperature distribution was evaluated. The thermal analysis was coupled to static structural analysis. For the structural analysis the rotating (aluminum) rod was brought to stationary and the forging pressure was applied on the brass rod along the axis of rod. The brass rod was allowed to move in the axial direction. The structural analysis was carried out for the equivalent stress and strain, total and directional deformation. The contact analysis was also carried out to estimate the depth of penetration and sliding of the material at the interface.

The analysis of friction welding was carried out as per the design of experiments using Taguchi techniques. The process parameters and their levels are given table-1. The orthogonal array (OA), L9 was selected for the present work. The parameters were assigned to the various columns of O.A. The assignment of parameters along with the OA matrix is given in Table 2.

Table 1: Process parameters and levels

Factor	Symbol	Level–1	Level–2	Level–3
Frictional Pressure, MPa	A	20	30	40
Frictional time, Sec	B	4	5	6
Rotational speed	C	1000	1250	1500
Forging pressure, MPa	D	25	37.5	50

Table 2: Orthogonal Array (L9) and control parameters

Treat No.	A	B	C	D
1	1	1	1	1
2	1	2	2	2
3	1	3	3	3
4	2	1	2	3
5	2	2	3	1
6	2	3	1	2
7	3	1	3	2
8	3	2	1	3
9	3	3	2	1

3. Results and Discussion

The temperature distribution from the transient thermal analysis; equivalent stress and directional deformation from the structural analysis; penetration and sliding from the contact analysis are discussed in the following sections.

Table 3: ANOVA summary of the temperature distribution

Source	Sum 1	Sum 2	Sum 3	*SS*	*v*	*V*	*F*	*P*
A	1996	2867	3730	250683	2	125341.5	13070.02	71.45
B	2697	2828	3068	11780	2	5889.91	614.17	3.35
C	2358	2885	3350	82028	2	41014.21	4276.77	23.38
D	3008	2848	2736	6255	4	1563.82	163.07	1.77
e				67	7	9.59	1	0.05
T	10059	11427	12883	350814	17			100

Note: *SS is the sum of square, v is the degrees of freedom, V is the variance, F is the Fisher's ratio, P is the percentage of contribution and T is the sum squares due to total variation.*

3.1 Influence of Parameters on Temperature Distribution

Table – 3 gives the ANOVA (analysis of variation) summary of raw data. The Fisher's test column establishes all the parameters (A, B, C and D) accepted at 90% confidence level. The percent contribution indicates that the friction pressure, A contributes 71.45% of variation, B (friction time) aids 3.35% of variation, C (rotational speed) influences 23.38% of variation and D (forging pressure) contributes 1.77% of variation on the temperature distribution. The effect of forging pressure is due to reaction of frictional pressure.

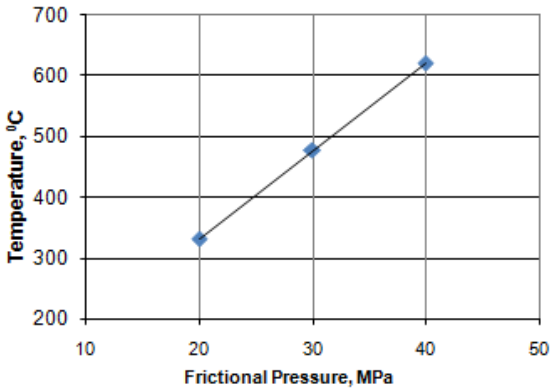

Figure 6: Influence of frictional pressure on temperature.

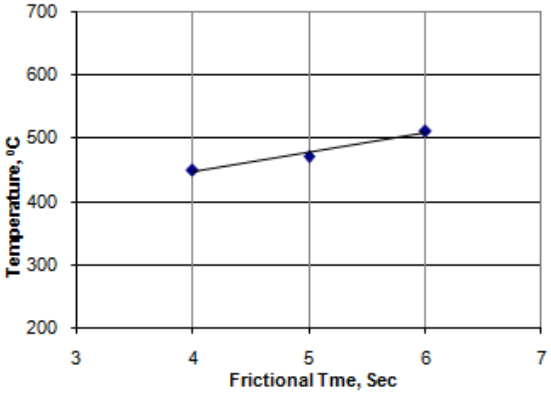

Figure 7: Influence of frictional time on temperature.

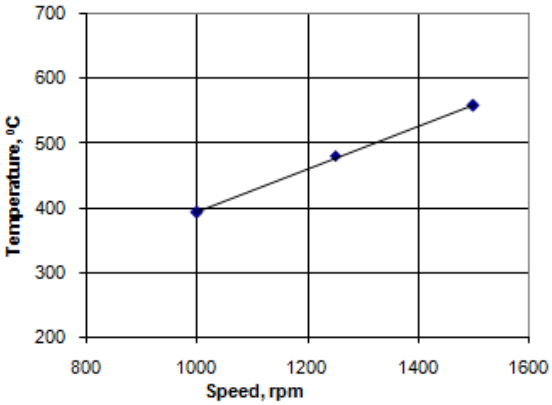

Figure 8: Influence of rotational speed on temperature.

The temperature developed in the welding rods is directly proportional to the frictional pressure, frictional time and rotational speed as shown in figure 6, 7 & 8. In fact this is natural phenomena. Form figure 9 it is observed that the temperature is very high at the interface. The trial 9 gives the highest temperature generation and trial 1 gives the lowest temperature generation in the rods. Change of temperature field is generated by heat flux that depends on: frictional pressure on the contact surface, relative velocity of the two faces, frictional time and coefficient of friction.

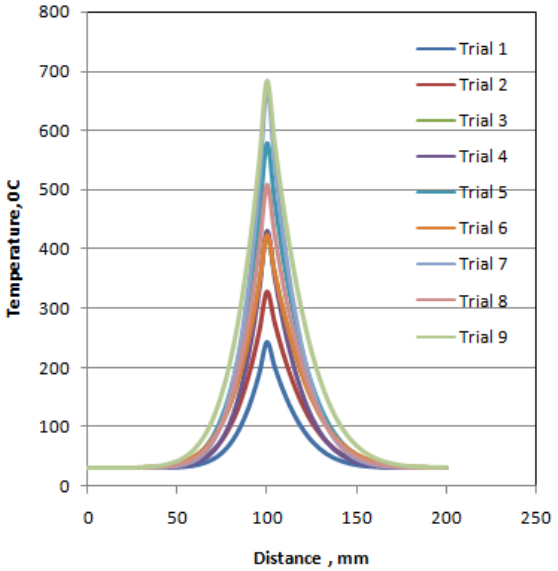

Figure 9: Temperature distribution during different trials

Table 4: ANOVA summary of the equivalent stress

Source	Sum 1	Sum 2	Sum 3	*SS*	*v*	*V*	*F*	*P*
A	575.18	852.42	1068.58	20390.86	2	10195.43	1321.78	91.48
B	775.80	846.35	874.026	855.07	2	427.535	55.43	3.77
C	787.59	859.38	849.206	502.98	2	251.49	32.60	2.19
D	870.73	795.77	829.676	469.68	4	117.42	15.22	1.97
e				53.99	7	7.713381	1.00	0.59
T	3009.3	3353.92	3621.488	22272.58	17			100

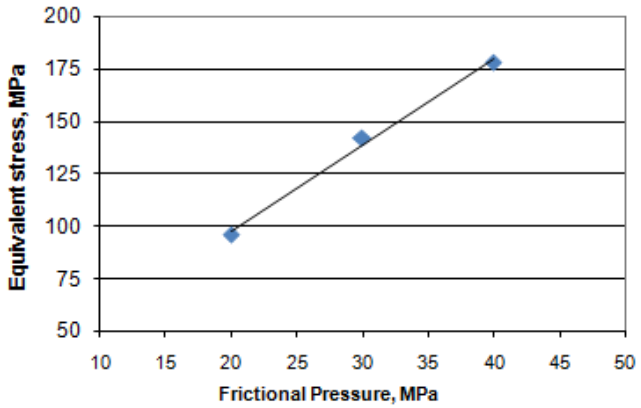

Figure 10: Influence of frictional pressure on equivalent stress.

3.2 Influence of parameters on equivalent stress

The ANOVA summary of the elastic modulus is given in Table 4. The Fisher's test column ascertains all the parameters (A, B, C, D) accepted at 90% confidence level influencing the variation in the equivalent stress. The major contribution (91.48%) is of friction pressure towards variation in the effective stress. The influence of other factors is negligible.

The equivalent stress increases with an increase in the frictional pressure as shown in figure 10. It is observed from table 5 that the equivalent stress is maximum (194.66 MPa) for trail 9 at the end of frictional heating and is 167.52 MPa at the end of forging pressure. It is also observed from table 5 that the equivalent stress is maximum (84.46 MPa) for trail 1 at the end of frictional heating and is 52.84 MPa at the end of forging pressure. During friction heating stage any surface irregularities are removed, the temperature increases in the vicinity of the welded surfaces, and an interface of visco-plastic aluminum is formed. During forging pressure stage there is significant thermo-plastic deformation of aluminum in the contact area. In result of this is formation of a flange-like flash. The process of welding takes place due to the plastic and diffusion effects.

Table 5: Equivalent stress values under different trials

	At end of frictional heating	At end of forging
1	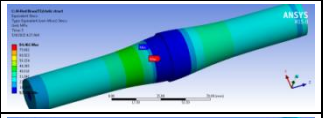	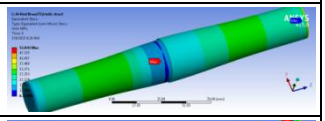
2	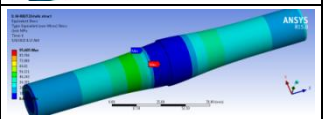	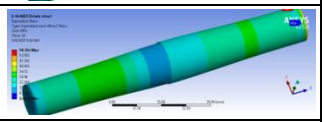
3	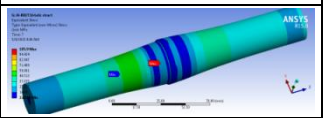	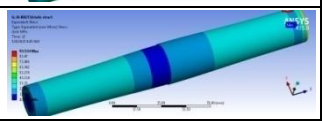
4	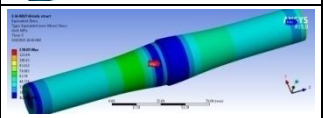	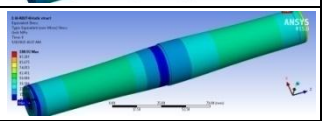
5	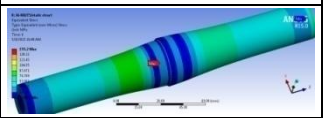	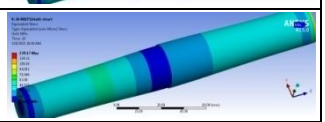
6	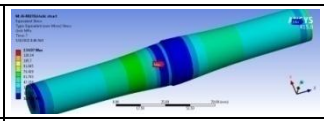	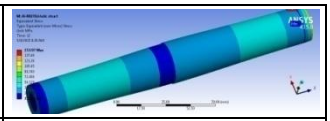
7	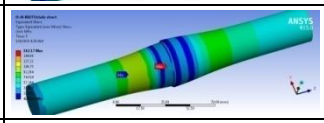	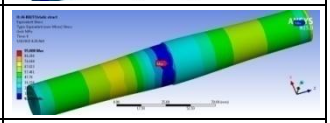
8	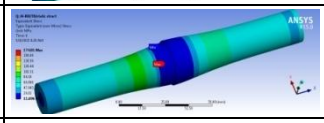	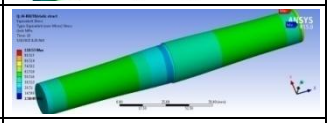
9	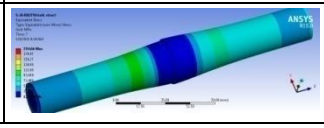	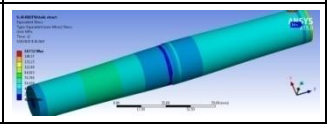

Table 6: ANOVA summary of the directional deformation

Source	Sum 1	Sum 2	Sum 3	*SS*	*v*	*V*	*F*	*P*
A	1.10953	1.76084	2.11739	0.1	2	0.05	55.64	62.18
B	1.37565	1.63511	1.977	0.04	2	0.02	22.25	25.53
C	1.30703	1.70164	1.97909	0.03	2	0.015	16.69	19.42
D	1.81637	1.61347	1.55792	0	4	0	0.00	2.2
e				-0.00629	7	-0.0009	1.00	-9.33
T	5.60858	6.71106	7.6314	0.16371	17			100

3.3 Influence of parameters on total deformation

The ANOVA summary of the directional deformation is given in Table 6. The Fisher's test column ascertains all the parameters (A, B, C, D) accepted at 90% confidence level influencing the variation in the directional deformation. The major contribution (38.18%) is of frictional pressure and frictional time towards variation in the directional deformation. The influence of rotational speed and forging pressure are 26.20% and 16.45% respectively.

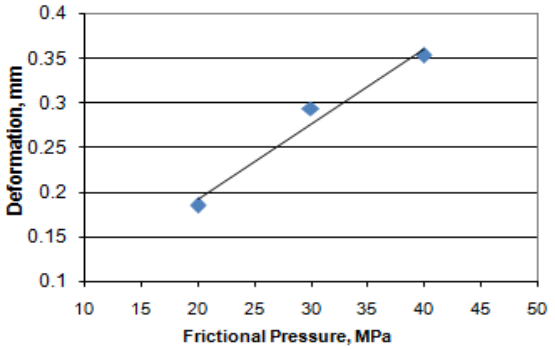

Figure 11: Influence of frictional pressure on deformation

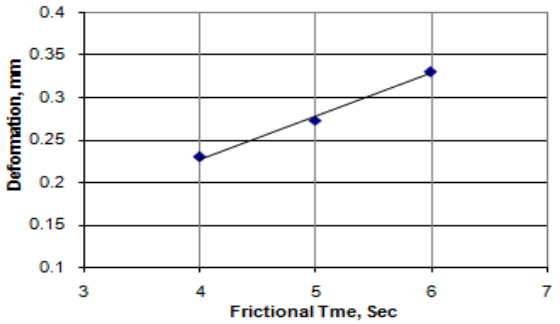

Figure 12: Influence of frictional time on deformation

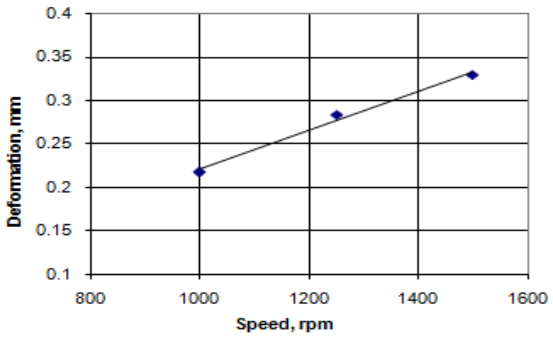

Figure 13: Influence of rotational speed on deformation

The total deformation increases with an increase in the frictional pressure, frictional time and rotational speed as shown in figure 11, 12 & 13. In the first numerical iteration (thermal) the external load generates uniform pressure on the contact surface and consequently linearly changing heat flux. In the next iteration (static) the forging pressure on the contact surface forces the material to penetrate and slid. It is observed that the deformation concentrates mainly near the frictional surface. The extruded shape gradually forms near the welded joint during the welding process. The extruded shape is asymmetric, as shown in table 6. It results from non-uniform material properties along the radial direction of the specimen during welding.

Table 6: Directional deformation values under different trials

	At end of frictional heating	At end of forging
1	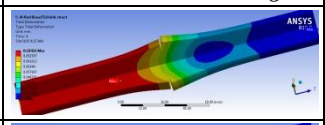	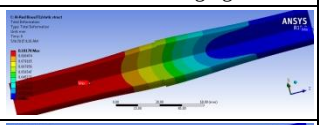
2	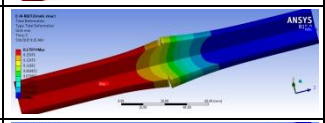	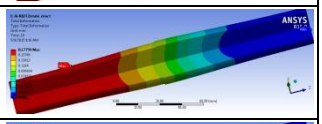
3	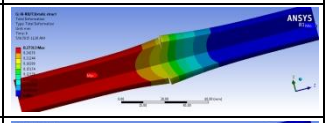	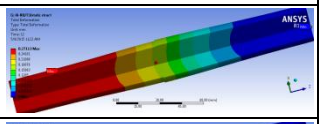
4	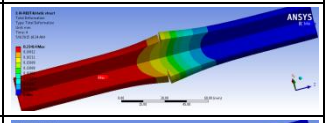	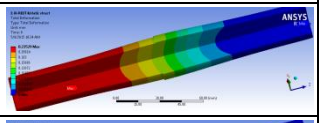
5	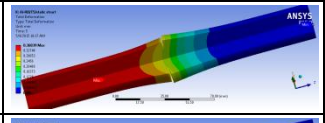	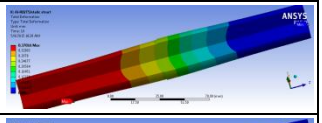
6	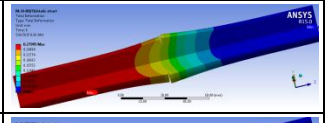	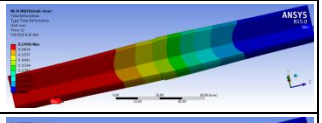
7	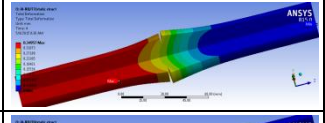	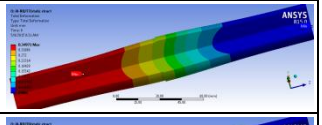
8	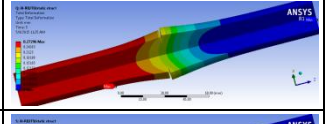	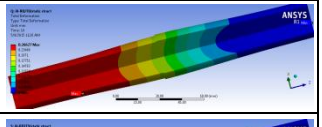
9	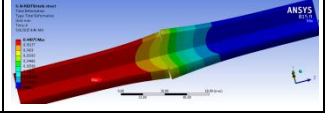	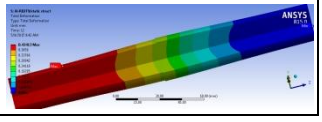

3.4 Influence of parameters on penetration and sliding

In friction welding of 2024Al and UNS C23000 brass, only 2024Al is consumed in the form of flash due to softer material as most of the heat generated at the interface is transferred to 2024Al. The deformation of UNS C23000 brass is negligible due to its higher hardness value, and higher melting point as shown in table 7. In the case of trail 1 the interface layer has not produced a good metallic bond between aluminum and brass. In the case of trail 7 & 9 the interface layer has produced a good metallic bond between aluminum and brass. A closer look at the penetration and sliding images shows that the failure of good bonding has taken place largely by interface separation. Some problems, such as inconsistency of the weld results, are encountered with this combination of materials. One factor may be the randomly varying relative motions between welding parts, which results in an uneven rate of heat generation. Due to this uneven rate of heat input, the amount of melt-off for each cycle for welding this combination of brass and aluminum.

The penetation of trials 7 and 9 are respectively 0.00167 and 0.00140 mm at the end of forging cycle. The slding of trials 7 and 9 are 0.015 and 0.016 mm respecticely. The optimal process parameters for 2024Al and UNS C23000 brass are found to be frictional pressure of 40 MPa, frictional time of 4 sec, rotational speed of 1500 rpm and forging pressure of 37.5 MPa. For this dissimilar metals of aluminium and brass, the forging pressure should be lesser than the frictional pressure. this is because of softness and high thermal properties. The heat generated due friction is high enogh to bring these materials into visco-plastic state, therefore, the forging pressure should be lesser than the frictional pressure. The experimental fricitional welding validateds the the seventh trial conditions as shown in figure 14.

Table 7: Penetration and sliding values under different trials

	Penetration	Sliding
1	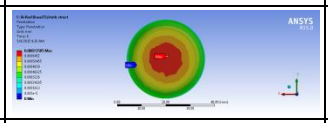	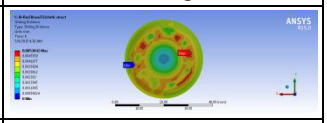
2	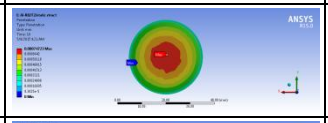	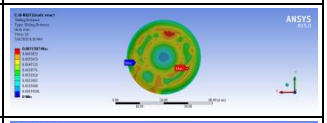
3	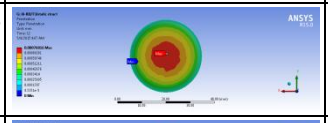	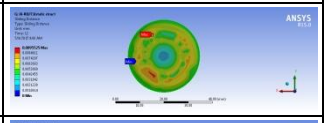
4	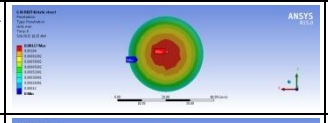	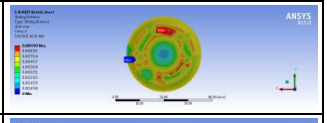
5	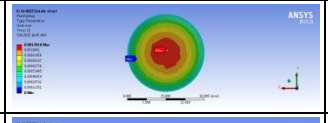	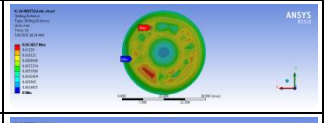
6	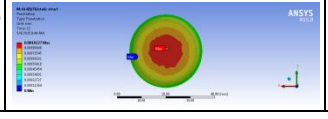	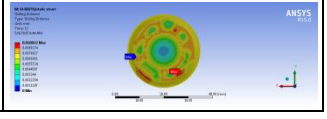

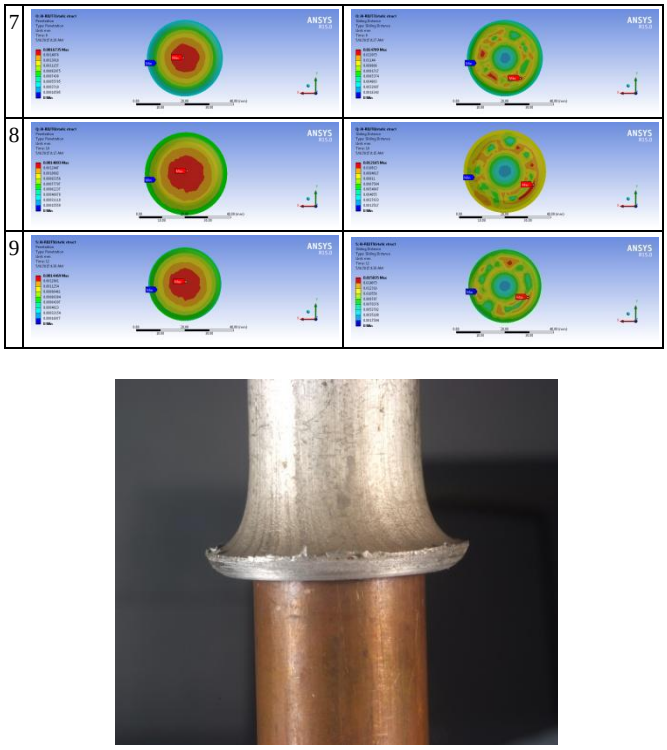

Figure 14: Welding aluminum and brass with trial 7 conditions.

4. Conclusions

This study shows that the 2024Al and b UNS C23000 brass is good if the operating conditions: frictional pressure of 40 MPa, frictional time of 4 sec, rotational speed of 1500 rpm and forging pressure of 37.5 MPa. For friction welding of brass and aluminum the forging pressure should be less than the frictional pressure or equal. For this condition of welding there was good penetration and sliding of materials at the welding interface resulting a good mechanical bonding. The equivalent stress was 162.70 MPa for this welding condition.

5. Acknowledgements

The author acknowledges with thanks University Grants Commission (UGC) – New Delhi for sectioning R&D project.

References

[1] A. Chennakesava Reddy, Fatigue Life Evaluation of Joint Designs for Friction Welding of Mild Steel and Austenite Stainless Steel, International Journal of Science and Research, vol.4, n0.2, pp. 1714-1719, 2015.
[2] A. Chennakesava Reddy, Fatigue Life Prediction of Different Joint Designs for Friction Welding of 1050 Mild Steel and 1050 Aluminum, International Journal of Scientific & Engineering Research, vol.6, no.4, pp. 408-412, 2015.
[3] B.S. Yibas, A.Z. Sahin, N. Kahrama, and A.Z. Al-Garni, "Friction welding of St-A1 and A1-Cu materials", Journal of Materials Processing Technology", (49), pp.431-443, 1995.
[4] A. Chennakesava Reddy, A. Ravaivarma, and V. Thirupathi Reddy, in Proceedings of National Welding Seminar, IIT-Madras, pp.51-55, 2002.
[5] W. Li and F. Wang, "Modeling of continuous drive friction welding of mild steel", Materials Science and Engineering A, (528), pp.5921-5926, 2011.
[6] Chennakesava, R. Alavala, "CAD/CAM: Concepts and Applications," PHI Learning Pvt. Ltd, 2008:
[7] Chennakesava R. Alavala, "Finite element methods: Basic Concepts and Applications, PHI Learning Pvt. Ltd., 2009.